Molecular Dynamcis Study of Thermomechanical Behavior of WSe_2 (Tungsten Diselenide) for Flexible Wearable Sensors

Submitted By
MD. Ibrahim Hossain Khan - 200012105
Shadman Arif Rohan - 200012123

Supervised By
Dr. Mohammad Nasim

A Thesis submitted in partial fulfillment of the requirement for the degree of Bachelor of Science in Industrial and Production Engineering

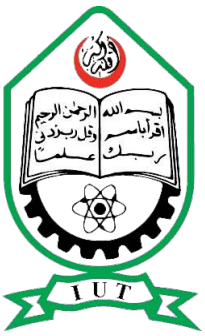

Department of Mechanical and Production Engineering (MPE)

Islamic University of Technology

29 September, 2025

Candidates' Declaration

It is to certify that the work presented in this thesis, titled, "Molecular Dynamics Study of Thermomechanical Behavior of WSe_2 (Tungsten Diselenide) for Flexible Wearable Sensors", is the outcome of the investigation and research carried out by me under the supervision of Dr. Mohammad Nasim, Assistant Professor, MPE, IUT.

It is also declared that neither this thesis nor any part of it has been submitted elsewhere for the award of any degree or diploma.

MD. Ibrahim Hossain Khan
Student No: 200012105

Shadman Arif Rohan
Student No: 200012123

Recommendation of the Thesis Supervisors

The thesis titled "Molecular Dynamics Study of Thermomechanical Behavior of WSe_2 (Tungsten diselenide) for Flexible Wearable Sensors" submitted by MD. Ibrahim Hossain Khan, (Student No: 200012105) and also Shadman Arif Rohan (Student ID: 200012123) has been accepted as satisfactory in partial fulfillment of the requirements for the degree of BSc. in Industrial and Production Engineering on September 29th, 2025.

04/12/25

Dr. Mohammad Nasim
(Superviser)
Assistant Professor
MPE Dept., IUT, Board Bazar, Gazipur-1704, Bangladesh

CO-PO Mapping of ME 4800 - Theis and Project

COs	Course Outcomes (CO) Statement	(PO)	Addressed by	
CO1	Discover and Locate research problems and illustrate them via figures/tables or projections/ideas through field visit and literature review and determine/Setting aim and objectives of the project/work research in specific, measurable, achievable, realistic and timeframe manner.	PO2 Problem analysis	Thesis Book	√
			Performance by research	√
			Presentation and soft skill	√
CO2	Design research solutions of the problems towards achieving the objectives and its application. Design systems, components or processes that meets related needs in the field of mechanical engineering	PO3 Design/development of solutions	Thesis Book	√
			Performance by research	√
			Presentation and soft skill	
CO3	Review, debate, compare and contrast the relevant literature contents.Relevance of this research/study. Methods, tools, and techniques used by past researchers and justification of use of them in this work.	PO4 Investigation	Thesis Book	√
			Performance by research	√
			Presentation and soft skill	
CO4	Analyse data and exhibit results using tables, diagrams, graphs with their interpretation. Investigate the designed solutions to solve the problems through case study/survey study/ experimentation/simulation using modern tools and techniques.	PO5 Modern tool usage	Thesis Book	√
			Performance by research	
			Presentation and soft skill	√
CO5	Apply moral values and research/professional ethics throughout the work, and justify genuine referencing on sources, and demonstration of own contribution.	PO8 Ethics	Thesis Book	√
			Performance by research	
			Presentation and soft skill	
CO6	Perform own self and manage group activities from the beginning to the end of the research/ work as a quality work.	PO9 Individual work and teamwork	Thesis Book	√
			Performance by research	√
			Presentation and soft skill	√
CO7	Compile and arrange the work outputs, write the report/thesis, a sample journal paper, and present the work to wider audience using modern communication tools and techniques.	PO10 Communication	Thesis Book	√
			Performance by research	√
			Presentation and soft skill	
CO8	Recognize the necessity of life-long learning in career development in dynamic real-world situations from the experience of completing this project.	PO12 Life-long learning	Thesis Book	√
			Performance by research	
			Presentation and soft skill	√

Student Name/ID:

1. **Md. Ibrahim Hossain Khan** - 200012105

2. **Shadman Arif Rohan** - 200012123

Signature of the Superviser _____

Name of The Superviser: Asst. Prof. Dr. Mohammad Nasim

K-P-A Mapping of ME 4800 -Theis and Project

COs	POs	Related Ks								Related Ps							Related As				
		K 1	K 2	K 3	K 4	K 5	K 6	K 7	K 8	P 1	P 2	P 3	P 4	P 5	P 6	P 7	A 1	A 2	A 3	A 4	A 5
CO1	PO2	√	√	√	√					√											
CO2	PO3					√				√	√	√				√	√	√	√		
CO3	PO4								√	√	√	√					√	√			
CO4	PO5						√			√				√							
CO5	PO8							√													
CO6	PO9																				
CO7	PO10																				
CO8	PO12																				

Student Name/ID:

1. **Md. Ibrahim Hossain Khan** - 200012105 Signature of the Superviser
2. **Shadman Arif Rohan** - 200012123 **Name of The Superviser: Prof. Dr. Mohammad Nasim**

Acknowledgement

We would like to express our heartfelt gratitude to Mr. Sifat Abdul Bari, Lecturer, for his constant support, insightful guidance, and encouragement throughout this research. His expertise in simulation and materials modeling was instrumental in shaping the direction of this work. We are also thankful for his time, patience, and valuable feedback during every step of the project.

Abstract

Among two-dimensional (2D) materials, transition metal dichalcogenides (TMDs) stand out for their exceptional electrical, optical, and mechanical properties, with tungsten diselenide (WSe_2) being a particularly promising candidate for next-generation nanoelectromechanical and flexible devices. However, imperfections such as pits, which frequently arise during synthesis or device fabrication, act as crack initiators that degrade the intrinsic mechanical stability and compromise device reliability. In this study, we employ molecular dynamics (MD) simulations to investigate the fracture response of monolayer WSe_2 nanosheets containing circular and triangular pit defects under uniaxial tensile loading along both armchair and zigzag orientations. Using the Stillinger–Weber (SW) interatomic potential within LAMMPS at a strain rate of 10^8 s^{-1} and room temperature (300 K), we analyze stress–strain behavior, crack initiation, and propagation mechanisms. The results show that the zigzag orientation provides superior mechanical resistance, with circular pits achieving a maximum yield strength of about 4.08 GPa at 6.0% strain, whereas triangular pits fractured earlier at around 3.00 GPa and 4.8% strain. In the armchair direction, circular pits reached approximately 3.55 GPa at 6.3% strain, while triangular pits failed at 3.06 GPa and 4.0% strain. Results reveal the anisotropic nature of WSe_2 and demonstrate that both defect geometry and loading direction significantly alter mechanical performance. This work provides fundamental insights into defect-driven fracture mechanisms in WSe_2, offering useful guidelines for the design and reliability assessment of TMD-based nanodevices.

Summary

The semiconductor industry has been moving towards materials that are thinner, faster, and more efficient than traditional silicon. Among these, two-dimensional (2D) materials—which are only a few atoms thick—have attracted enormous interest because they can combine high electrical performance with mechanical flexibility. A particularly promising family of these materials is the transition metal dichalcogenides (TMDs), and within this family, tungsten diselenide (WSe_2) stands out for its excellent electronic, optical, and mechanical properties. These features make WSe_2 a strong candidate for use in flexible electronics, transistors, sensors, and other next-generation semiconductor devices.

However, one of the key challenges is that during material growth and device fabrication, tiny imperfections known as pits can form in the WSe_2 sheet. Although these pits are on the nanoscale and invisible to the naked eye, they can act as weak points where cracks begin to grow. Over time, this can lead to device failure, reducing efficiency, reliability, and overall productivity. Understanding how these defects affect the strength of the material is therefore crucial for ensuring the durability of devices built from WSe_2.

In this thesis, we used molecular dynamics (MD) simulations—a computer-based method that models atoms and their interactions—to study how WSe_2 behaves when defects are present. We specifically created two common pit shapes, circular and triangular, in a nanosheet of WSe_2 and then applied stretching forces along the two main directions of its atomic structure, known as the zigzag and armchair orientations. By doing so, we were able to observe in detail how cracks initiate, how they spread, and under what conditions the nanosheet eventually breaks.

Our findings showed that both the direction of loading and the geometry of the pit strongly influence how the nanosheet fails. Circular pits were found to distribute stress more evenly and could withstand greater forces before breaking, while triangular pits concentrated stress at

their sharp corners, leading to earlier crack formation. Furthermore, nanosheets stretched in the zigzag direction were able to endure higher stresses compared to those stretched in the armchair direction, highlighting the material's anisotropic (direction-dependent) properties.

These insights are important for the semiconductor industry because they highlight how the presence of defects can compromise the performance of WSe_2-based devices. By understanding which types of defects are most damaging and how the material behaves under stress, engineers can design more reliable, defect-tolerant devices and optimize fabrication techniques to minimize harmful imperfections. Ultimately, this research supports the development of stronger and more durable flexible electronics, ensuring that future semiconductor technologies built with WSe_2 can achieve both high performance and long operational lifetimes.

Table of Contents

List of Figures

List of Tables

Chapter 1

Introduction

1.1 Overview

The shift from conventional silicon to two-dimensional (2D) materials was motivated by the limitations of traditional semiconductors, notably graphene's lack of a bandgap, which restricts its utility in field-effect transistors (FETs) and nanoelectronics. Transition metal dichalcogenides (TMDs), characterized by a tunable direct bandgap and mechanical flexibility, have emerged as viable alternatives for flexible and wearable devices. Among these, WSe_2 is of special interest because it exhibits ambipolar conducting behaviors, enabling the construction of all p-type and n-type complementary digital logic circuits on a single nanosheet [3, 2]. FETs based on WSe_2 demonstrate a very high I_{ON}/I_{OFF} ratio of approximately 10^8, and the material also exhibits exceptionally low thermal conductivity, measuring $\sim$ 0.05 W m^{-1} K^{-1} cross-plane and $\sim$ 1.5 W m^{-1} K^{-1} in-plane 187. These properties, combined with its suitable bandgap ($\sim$ 1.67 eV) and confirmed use in flexible, transparent, and ultra-broadband photodetectors for wearable devices, underscore the critical importance of understanding its mechanical reliability under strain, especially when defects like pits are present.

1.2 Objectives of the Study

The aim of this work is to investigate the mechanical behavior and fracture mechanisms of pristine and defected tungsten diselenide (WSe_2) monolayers using molecular dynamics simulations.

The specific objectives are:

1. To develop and optimize an atomistic model of monolayer WSe_2 incorporating nanoscale pit defects.

2. To evaluate the mechanical properties of WSe_2 under uniaxial tensile loading along zigzag and armchair directions.

3. To identify the crack initiation and propagation mechanisms in pristine and pitted WSe_2 nanosheets.

1.3 Structure of the Thesis

Chapter 1: Introduction

This chapter presents the significance of WSe_2 as a two-dimensional transition metal dichalcogenide (TMD) material with favorable mechanical and thermal properties. It highlights the growing need for wearable and flexible electronics and emphasizes the significance of molecular dynamics (MD) simulations in explaining nanoscale material behavior under mechanical and thermal stress.

Chapter 2: Literature Review

This chapter summarizes key previous research works on WSe_2 and other TMDs, focusing on their mechanical behavior, cracking mechanisms, and electronic applications. Research gaps are identified—especially the lack of simulation-based exploration of crack propagation in nanosheets under various strain rates and loading directions.

Chapter 3: Description of the Model/System

This chapter defines the atomic model of the WSe_2 nanosheet used in the simulations, including its lattice structure, orientation (armchair and zigzag), and size. It also explains how the model was created using programs like Atomsk and prepared for input into LAMMPS.

Chapter 4: Computational Methodology

This chapter details the simulation setup in LAMMPS, including boundary conditions, ensemble options (NPT and NVT), strain rates, and timestep values. The interatomic potential used to model atomic forces is described, along with the setup of output parameters such as stress, strain, and atomic positions for subsequent analysis.

Chapter 5: Results and Discussions

This chapter presents and discusses the simulation results—stress–strain curves, deformation modes, and crack growth behavior under different strain rates and tensile loading directions. The influence of directionality (zigzag or armchair) and strain rate on fracture behavior is analyzed, and the findings are correlated with practical device design applications.

Chapter 6: Conclusion

This chapter concludes the study by summarizing the main findings, confirming that the mechanical properties of WSe_2 are highly sensitive to strain rate and loading direction. It also discusses the potential of WSe_2 for wearable electronics and suggests directions for future research, including more comprehensive material comparisons and industrial integration opportunities.

Chapter 2

Literature Review

2.1 Quantitative Context of Structural Phase Stability

The mechanical investigation of WSe_2 must be contextualized by acknowledging its structural phase dependence, as the material can exist in the high-strength trigonal prismatic phase (h-WSe_2) or the metastable distorted octahedral coordinated phase (t-WSe_2). Studies focusing on these intrinsic structures reveal massive disparities in mechanical performance, which directly impacts device reliability. For instance, h-WSe_2 exhibits substantially superior tensile properties: under uniaxial loading (300 K, 1×10^{-4} ps^{-1}), the h-phase demonstrates a fracture strength of 16.20 GPa and a Young's modulus of 119.73 GPa along the armchair direction. In sharp contrast, the corresponding mechanical properties for the t-phase are significantly deteriorated, yielding a much lower fracture strength of 3.46 GPa and a Young's modulus of 68.57 GPa in the same orientation. This dramatic difference confirms that the structural stability of the thermodynamically favorable h-phase is a prerequisite for achieving the necessary mechanical robustness in WSe_2-based flexible wearable sensors.

2.2 Investigation of the mechanical properties and fracture mechanisms of graphene/WSe_2 vertical heterostructure: A molecular dynamics study

Tungsten diselenide (WSe_2), a two-dimensional (2D) transition metal dichalcogenide, has high demand due to its flexibility and mechanical properties, which together make it a good material for flexible wearable sensors. Molecular dynamics (MD) simulations are the basic technique through which it is possible to find out the thermomechanical behavior of the strain and tem-

perature condition that the material goes through. To investigate thermo-mechanical properties, Gautam et al. (2024) on the tensile properties and fracture mechanisms of the graphene/WSe_2 vertical heterostructures, and the obtained information shed light on the performance of WSe_2 [6].

Strengths

- The work demonstrates that WSe_2's tensile strength is improved in the heterostructure configuration, which in turn highlights the regnant feature of sensor durability.
- By specifying the temperature change in the mechanical characteristics of the material, the work paves the way for creating wearable sensors that can be used under various conditions.
- Chowdhury et al. (2021) [2] presents an approach to guide the material selection to a sensor's most appropriate use through the fracturing mechanism that is determined by the helicity of the structure.

Gaps

- The analysis is limited to the thermomechanical properties of WSe_2 in heterostructures only, which are not directly suitable for wearable sensors made solely of WSe_2.
- Chowdhury et al. (2021) [2] did not analyze the existence of defects (e.g., vacancies) that will have negative effects on the flexibility of WSe_2 [5].
- They do not bring up the computational cost and model interpretability.

This research confirms the main idea of the paper by illustrating WSe_2's flexibility in the sensor domain and, at the same time, it proposes further molecular modeling (FMM) on WSe_2 and defect effects to be developed for the enhancement of thermomechanical performance through autonomous research.

2.3 Flexible, transparent and ultra-broadband photodetector based on large-area WSe_2 film for wearable devices

Tungsten diselenide (WSe_2), a type of two-dimensional (2D) transition metal dichalcogenide, is a material that shows great promise for flexible wearable sensors because of its mechanical

flexibility and optoelectronic properties. In a study by Zheng et al. (2016) [9], which reported the development of a flexible, transparent, ultra-broadband photodetector using large-area WSe_2 films grown via pulsed laser deposition (PLD), WSe_2's potential for wearable sensor applications was clearly demonstrated. The study reported WSe_2 films with an average transparency of 72% in the visible range and photoresponse from 370 to 1064 nm, achieving a responsivity of 0.92 A W^{-1}, external quantum efficiency of 180%, and a response time of 0.9 s. The device also exhibited excellent mechanical flexibility and air stability, maintaining performance after bending, which supports the focus of this thesis on WSe_2's thermomechanical behavior for flexible sensor applications [9].

Strengths

- WSe_2's flexibility and durability are demonstrated, supporting its suitability for bendable sensor designs.
- The study achieves a wide range of broadband response, increasing WSe_2's versatility for wearable optoelectronic devices.
- The quality of PLD-grown WSe_2 is well reported and characterized.

Gaps

- The study does not investigate the thermal stability of WSe_2, a key issue for sensor reliability (Fadeel et al., 2024) [5].
- There is a lack of information regarding WSe_2's mechanical performance under varying strain and temperature conditions.
- The report provides limited discussion on issues impacting WSe_2's performance in flexible devices.

This research highlights the performance of WSe_2 in flexible sensor applications and emphasizes the need for molecular dynamics (MD)-based thermomechanical studies to further enhance WSe_2's performance in wearable devices.

2.4 Mechanical Properties of Atomically Thin Tungsten Dichalcogenides: WS_2, WSe_2, and WTe_2

Tungsten diselenide (WSe_2) is a two-dimensional (2D) material gaining attention for its flexibility and strength, making it a strong candidate for use in flexible wearable sensors. Understanding its performance under stress and heat is essential to ensure reliable sensor operation. A study by Falson et al. (2020) [4] investigated the mechanical properties of thin tungsten-based materials, including WSe_2, through both experimental testing and computational methods. The researchers found that WSe_2 possesses a Young's modulus of approximately 170 GPa and a breaking strength of around 12 GPa. These findings indicate that while WSe_2 is not as stiff as some other materials, it still exhibits significant strength. The study also noted that WSe_2 shows distinctive behavior under strain, especially when fractures begin to form at stress concentration points, an important observation for designing durable sensors.

Strengths

- Fadeel et al. (2024) provides clear quantitative values for WSe_2's stiffness and strength, supporting its suitability for flexible sensor applications.
- It identifies fracture initiation mechanisms under strain, which can guide improved sensor design.
- The paper combines both experimental and computational approaches, offering a comprehensive understanding of WSe_2's mechanical properties.

Gaps

- Fadeel et al. (2024) does not examine thermal properties, which are crucial for understanding sensor performance under varying temperature conditions [5].
- The study shows limited integration of molecular dynamics (MD) simulations, reducing its applicability to atomistic-level studies.
- It provides minimal discussion of defect impacts, which can significantly influence WSe_2's flexibility and overall performance.

This study demonstrates that WSe_2 is well-suited for flexible sensor applications but emphasizes the need for further investigation into its thermal response and defect-related behaviors to enhance its reliability in wearable technology.

Chapter 3

Model Development: Material & Methods

3.1 Precise Definition of Model Geometry and Defect Orientation

The monolayer nanosheet utilized throughout this study is defined by the thermodynamically favorable trigonal prismatic phase (h-WSe_2), where each tungsten (W) atom is covalently bonded to six selenium (Se) atoms within the layer. The construction of nanoscale pits rigorously accounts for the anisotropic mechanical response of the hexagonal lattice structure. Specifically, the equilateral triangular pits were strategically oriented relative to the crystallographic axes, mirroring meticulous protocols established in similar two-dimensional material studies (e.g., $MoTe_2$ with varying pit angles). For tensile loading applied along the armchair direction (X-axis), the base of the triangular pit was defined to lie parallel to the zigzag direction (Y-axis), ensuring that the pit's height (H) was aligned with the applied strain. Conversely, for tension along the zigzag direction (Y-axis), the pit's base (W) was aligned parallel to the armchair direction (X-axis). This precise orientation ensures a comparative analysis of how highly localized stress concentration points (the sharp pit corners) interact with the intrinsically anisotropic bond structure during mechanical failure.

3.2 Atomistic Model Development and Simulation Tools

The atomistic model of a tungsten diselenide (WSe_2) nanosheet was constructed using the Atomsk package. WSe_2 belongs to the family of transition metal dichalcogenides (TMDs) and crystallizes in a hexagonal lattice structure. The monolayer consists of a hexagonal arrangement where a plane of tungsten (W) atoms is sandwiched between two planes of selenium (Se) atoms, forming a trigonal prismatic coordination.

The starting point of the model development was the generation of a primitive unit cell of monolayer WSe_2, based on experimentally established lattice parameters. The unit cell was then systematically replicated along the x-, y-, and z-directions to create a larger supercell. This replication was necessary to build a nanosheet of sufficient size to capture realistic deformation characteristics and to minimize size-related artifacts during mechanical loading. The resulting supercell retains the atomic orientation of the unit cell, ensuring that crystallographic directions such as armchair and zigzag are preserved. These orientations are critical since they define the directions along which uniaxial tensile loads were later applied, thereby enabling the assessment of anisotropic mechanical properties.

In this study, a supercell of approximately 30 nm $\times$ 30 nm was constructed, providing a representative nanosheet size for deformation analysis while remaining computationally tractable. The model geometry ensures that boundary conditions and loading paths can be consistently imposed to study the mechanical response under uniaxial tensile deformation.

Tools Used and Their Roles

- **Atomsk:** Used to build the WSe_2 structure by replicating the unit cell into a larger supercell. Atomsk enables the generation of LAMMPS-readable data files for precise atomic modeling and structural definition.
- **LAMMPS (Large-scale Atomic/Molecular Massively Parallel Simulator) [1, 3]:** Employed to simulate the thermo-mechanical response of the WSe_2 nanosheet under various strain rates and tensile directions. It calculates essential physical quantities such as stress, strain, temperature, and potential energy at the atomic scale.
- **OVITO (Open Visualization Tool) [1, 2]:** Utilized for visualizing atomic motion, crack propagation, and structural deformation. OVITO aids in interpreting simulation results, including stress–strain behavior, defect evolution, and fracture mechanisms.

3.3 Identify the Unit Cell

The unit cell is the lowest periodic structure in a crystal that dictates the atomic arrangement and symmetry of the material. For tungsten diselenide (WSe_2), the unit cell adopts a hexagonal crystal structure corresponding to the space group $P6_3/mmc$. The lattice parameters and angles are given by $\alpha = \beta = 90^\circ$ and $\gamma = 120^\circ$. These structural parameters are crucial for accurately modeling the physical and mechanical behavior of the material.

The unit cell serves as the fundamental building block, and it is systematically replicated to form a larger supercell that mimics the behavior of nanosheets under mechanical loading. An accurately defined unit cell ensures reliable predictions in stress–strain analysis and simulations of crack initiation and propagation.

Crystallographic Details

Space Group: $P6_3/mmc$

Lattice Parameters:

- $a = b = 0.331$ nm
- $c = 1.298$ nm

Lattice Angles: $\alpha = \beta = 90°, \gamma = 120°$

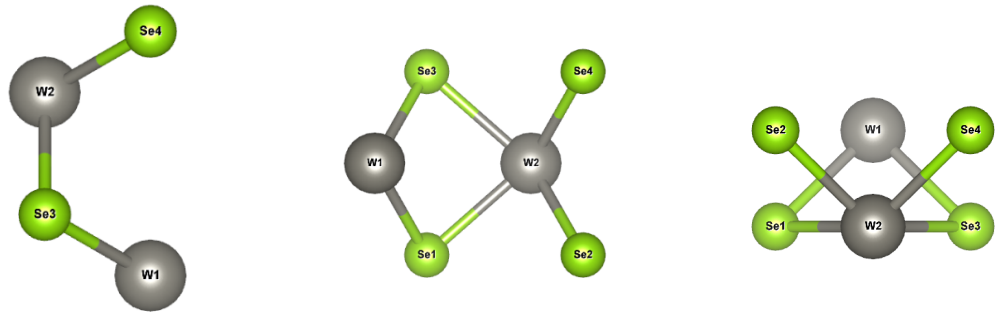

(a) ***xy Orientation*** (b) ***yz Orientation*** (c) ***xz Orientation***

Figure 3.1: Different Orientation of Unit cell

The Figure 3.1 shows the representation of a single h-WSe_2 unitcell in x-y, y-z and z-x plane.

Electronic band structure:

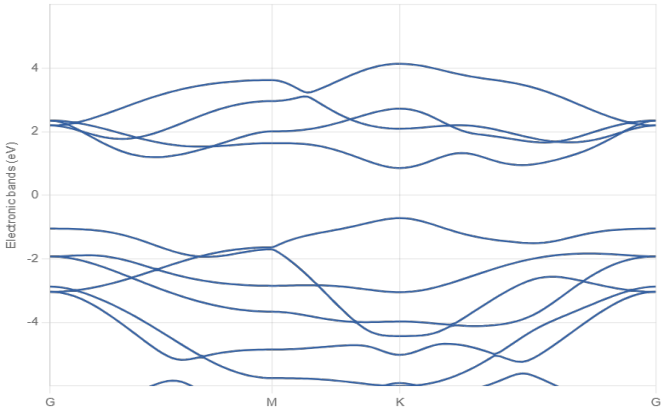

Figure 3.2: Electronic Band Structure (G-M-KG)

In the Figure 3.2, we are able to demonstate the elctronic band structure of h-WSe_2 (G-M-KG).

3.4 Atomistic Supercell Construction and Defect Engineering

The mechanical properties and fracture mechanisms of materials at the nanoscale are significantly influenced by finite size effects, necessitating the use of a sufficiently large simulation domain in Molecular Dynamics (MD) studies. To accurately capture realistic deformation behaviors and minimize boundary condition artifacts, the atomistic model was prepared by generating a large periodic supercell of monolayer Tungsten Diselenide (WSe_2).

3.5 Generate Supercell

To employ molecular dynamics (MD) simulations for investigating the mechanical behavior of a two-dimensional (2D) WSe_2 nanosheet, a sufficiently large atomic structure is required. To this end, the unit cell is duplicated to create a *supercell*, which contains an adequate number of atoms to accurately capture deformation, fracture, and thermal responses under applied stress.

In forming a structure that resembles a nanosheet, the supercell expands the unit cell along the x, y, and z axes while preserving atomic symmetry and bonding integrity. Since WSe_2 is a layered material, simulations are typically performed on a monolayer configuration by extending the structure in the x and y directions to form a planar sheet and minimizing the z-dimension.

To prevent spurious interactions between periodic images in the out-of-plane (z) direction, a vacuum gap is introduced. This ensures that interlayer forces do not affect the results and that the model behaves as an isolated 2D monolayer during simulation.

Software Tool: Atomsk

The supercell was generated using the `Atomsk` package, an open-source tool specifically designed for creating and manipulating atomic structures for simulation.

Supercell Dimensions and Configuration

A supercell of approximate dimensions 30 nm $\times$ 30 nm was constructed in the XY plane. The replication numbers were chosen to yield a system containing a sufficiently large number of atoms to represent a nanosheet under tensile loading.

Atomsk Command Structure for Supercell Generation

The process involved taking the WSe_2 unit cell (input file: `unitcell.xyz`) and replicating it along the crystallographic axes, then exporting the geometry directly to the format required by the simulation software (`LAMMPS`).

```
$ atomsk unitcell.xyz -duplicate Nx Ny 1 supercell.lmp
```

where `Nx` and `Ny` represent the necessary number of repetitions to achieve the ~ 30 nm dimensions along the X and Y axes, and the factor of 1 along the Z axis ensures a single monolayer. The resulting structure was composed of W and Se atoms in the correct 1 : 2 stoichiometric ratio (as shown in Figure 3.3).

Different Orientation of the nanosheet:

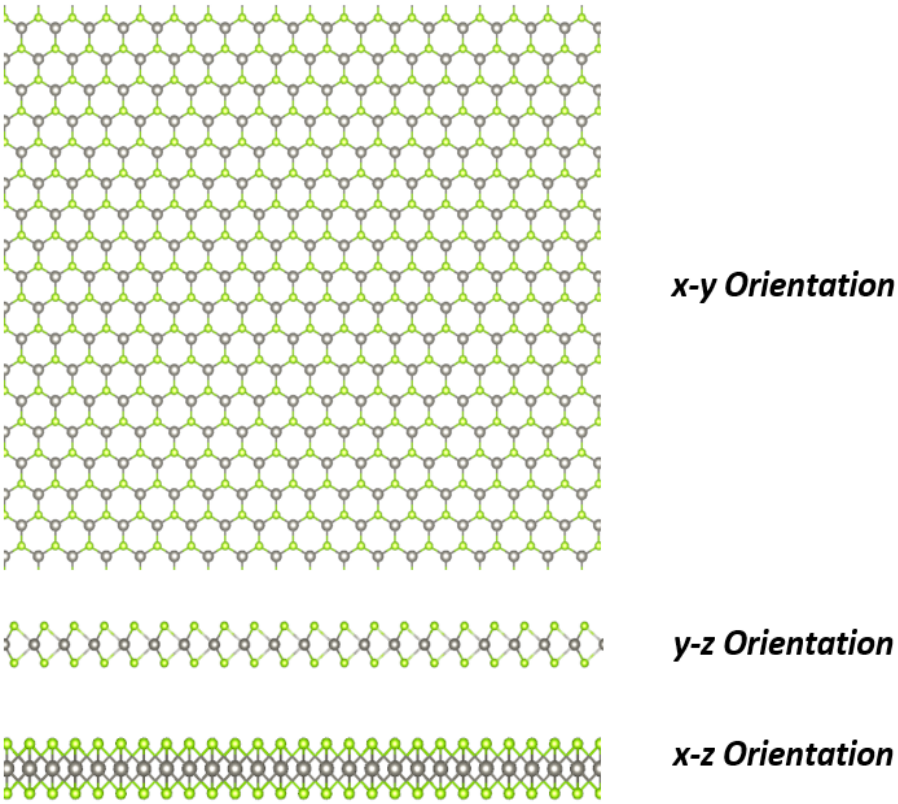

Figure 3.3: Different Orientation of the supercell

In the Figure 3.3, we are able to see the supercell of WSe_2 created in `Atomsk` software, showed in x-y, y-z and z-x directions.

Example of our 30nm x 30nm WSe_2 Nanosheet Supercell

To study the mechanical behavior of WSe_2 at the nanoscale, a supercell structure representing a monolayer nanosheet of approximately 30 nm × 30 nm was generated (as shown in Figure 3.4) [7]. The supercell was constructed by systematically replicating the crystal's unit cell multiple times along the x and y directions, ensuring periodic continuity and preservation of atomic symmetry.

This nanosheet model provides a sufficiently large simulation domain to capture the essential deformation, fracture, and crack propagation mechanisms that occur under tensile loading. The in-plane dimensions allow for realistic stress–strain behavior while maintaining computational efficiency.

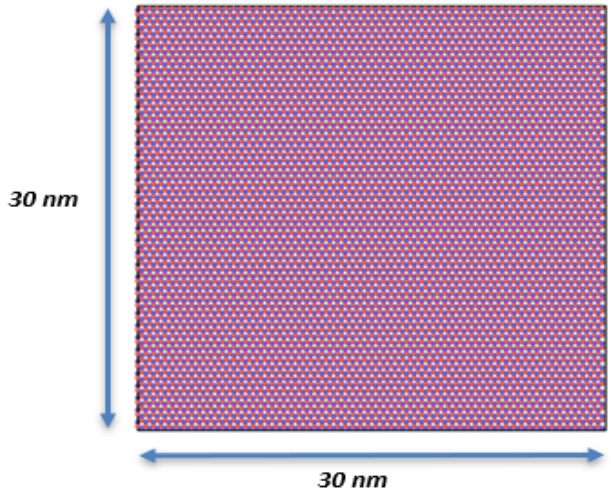

Figure 3.4: Simple nano sheet in Ovito software (30 × 30 nm)

Vacuum Layer and Boundary Conditions

To physically model the two-dimensional nature of the monolayer and eliminate non-physical cross-layer interactions due to periodic imaging, a vacuum gap was imposed along the out-of-plane Z direction. A vacuum spacing of ~ 1.5–2.0 nm (~ 15–20 Å) was introduced above and below the WSe_2 layer. Periodic boundary conditions (PBCs) were applied in the X and Y directions for the subsequent loading simulations.

3.6 Circular Pit Construction

The circular pit was constructed to model an isotropic void, a geometry hypothesized to promote more uniform stress distribution and superior strain tolerance compared to defects with sharp

features. This defect type was instrumental in establishing a baseline for mechanical stability in the presence of a through-hole void.

- **Software and Environment:** Defect modeling employed a specialized `Python` script running in Google Colab, leveraging the coordinate manipulation capabilities of the Atomic Simulation Environment (`ASE`) package.

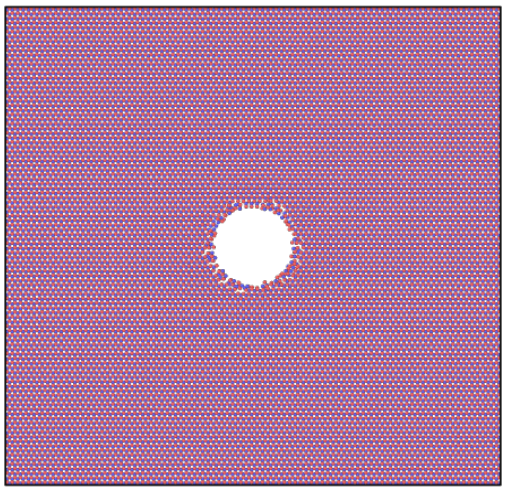

Figure 3.5: Circular Pit on the nanosheet

- **Geometric Definition:** A circular region with a precise diameter of **5** nm (50 Å) was mathematically defined. This corresponded to a fixed radius of 25 Å centered at the geometric midpoint of the WSe_2 nanosheet in the xy-plane (Figure 3.5).
- **Atom Deletion Criteria:** All Tungsten (W) and Selenium (Se) atoms whose in-plane coordinates fell strictly within the defined 25 Å radial boundary were selected for removal. A critical constraint was applied in the out-of-plane dimension (zzz-axis), requiring the atom's position to be within a designated 10 Å deletion slab to ensure the resultant structure was a clean, through-hole defect penetrating the entire monolayer thickness.
- **Mechanical Justification:** The curved boundary of the circular pit was expected to delay crack initiation, supporting the thesis finding that circular pits exhibit greater strain tolerance and stability compared to angular geometries.
- **Output Generation:** The final configuration, containing the well-centered 5 nm circular pit, was exported as a new `LAMMPS` data file for the subsequent tensile loading simulations.

3.7 Equilateral Triangular Pit Construction

The equilateral triangular pit (as shown on Figure 3.6) was engineered to simulate a sharp, anisotropic structural imperfection frequently found in synthesized TMDs. This geometry was specifically chosen to analyze the effects of highly localized stress fields, which are known to act as preferential sites for bond rupture and crack nucleation [1].

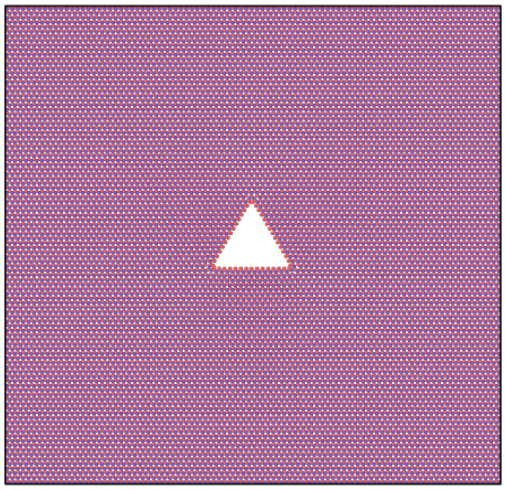

Figure 3.6: Triangular Pit on the nanosheet

- **Software and Environment:** Consistent with the circular pit, the triangular defect was generated using the customized `Python` script within the `ASE` environment.
- **Geometric Definition:** The pit was defined as an equilateral triangle with a uniform side length of 5 nm (50 Å). The coordinates of the vertices were precisely calculated from the centroid to ensure all interior angles were exactly 60° (Figure 3.6).
- **Orientation and Control:** Although an equilateral geometry was used in the WSe_2 thesis, related MD studies on $MoTe_2$ utilized isosceles triangular pits defined by parameters such as base (W), height (H), and a critical vertex angle (θ). These studies showed that mechanical properties are highly sensitive to the pit's orientation relative to the loading axes. A rotation parameter was therefore critical to align the pit along the desired crystallographic directions (armchair or zigzag).
- **Atom Deletion Criteria:** W and Se atoms were removed if their xy-coordinates fell strictly inside the triangular boundary and they resided within the 10 Å deletion slab along the zzz-axis. Verification of the strict equilateral geometry was performed prior to the final deletion step.

- **Mechanical Justification:** This sharp geometry was predicted to significantly lower the material's strength because angular geometries cause localized stress accumulation, which accelerates bond rupture and leads to premature crack initiation compared to circular voids. The resulting structure was then exported as a `LAMMPS` data file.

3.8 Loading Directions

The mechanical response of monolayer WSe_2 is fundamentally anisotropic due to the hexagonal symmetry of its crystal lattice. Therefore, to thoroughly characterize the thermomechanical behavior and fracture mechanisms of both pristine and defected nanosheets, uniaxial tensile loading was independently applied along the two principal crystallographic orientations. This approach is essential for providing foundational knowledge for advanced design strategies involving strain engineering in TMD-based devices.

Crystallographic Orientation and Loading Axes

The supercell was configured such that the primary crystallographic axes were aligned with the simulation box dimensions:

- **Armchair Orientation:** Tensile strain was applied along the X-axis (Figure 3.7(a)).
- **Zigzag Orientation:** Tensile strain was applied along the Y-axis (Figure 3.7(b)).

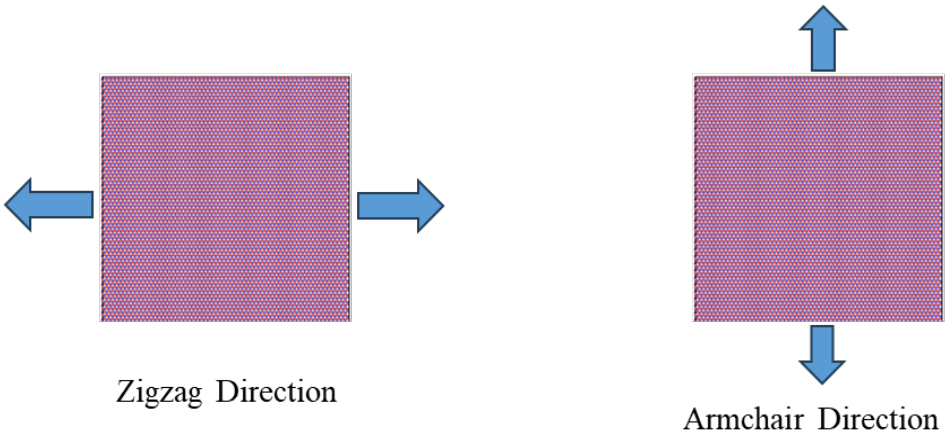

Figure 3.7: Different types of Loading on the nanosheet

These directions are critical because the bond arrangement and atomic coordination differ significantly between the zigzag axis, which follows a straight chain of bonds, and the armchair axis, which traverses alternating bond angles in a chair-like configuration.

Rationale for Anisotropic Testing

Testing along these two directions captures the directional dependency of mechanical performance and fracture behavior.

- **Anisotropy in WSe_2:** While bare (pristine) WSe_2 is generally reported to be more resilient to fracture along the armchair direction, the presence of nanoscale pits can significantly alter the failure mechanism. The present study demonstrated that the zigzag orientation provides superior mechanical resistance for the defected WSe_2 nanosheets, highlighting the non-trivial influence of pit geometry on intrinsic material anisotropy.
- **Defect-Specific Loading:** The orientation of the applied strain relative to the pit geometry is paramount. For example, in analogous studies on $MoTe_2$ with triangular pits, the base (W) of the pit was aligned either parallel to the armchair axis (for "X°" systems) or parallel to the zigzag axis (for "Y°" systems). During uniaxial tensile loading, the strain was applied along the axis parallel to the base (W) of the triangular pit.

The study exclusively applied uniaxial tensile loading for the WSe_2 nanosheets to evaluate the mechanical properties in conditions relevant to flexible and stretchable electronics.

Chapter 4

Computational Methodology

4.1 LAMMPS: Interatomic Potential and Stress Calculation

Interatomic Potential Selection (Stillinger–Weber) [1, 3, 8]

The atomic interactions within the WSe_2 monolayer were governed by the Stillinger–Weber (SW) interatomic potential, specifically the parameterization developed by Jiang et al. The SW potential is critical for accurately modeling WSe_2 because it incorporates both bond-stretching and angle-bending terms essential for 2D TMD materials. The selection of the SW potential is validated across multiple studies on TMDs, including those modeling WSe_2 mechanical reliability and similar defect studies on $MoTe_2$. This potential is preferred for its computational efficiency over alternatives like the Tersoff potential, while still accurately characterizing the mechanical properties of 2D TMDs.

- **Governing Equation:** The total energy ϕ of the system is a summation of two-body (V_2) and three-body (V_3) interactions:

$$\phi = \sum_{i<j} V_2 + \sum_{i>j<k} V_3 \tag{4.1}$$

- **Two-Body Term (V_2):** Models bond stretching and repulsion.
- **Three-Body Term (V_3):** Models angle bending, crucial for maintaining the trigonal prismatic coordination and reproducing the elastic response. The incorporation of the V_3 term is vital for accurately simulating the deformation of the layered WSe_2 structure.

Stress and Strain Formalism

- **Stress Calculation:** Global stress components were calculated at every timestep using the Virial stress theorem. Since 2D materials are modeled without considering the true bulk thickness, the resulting stress unit is reported as N/m, rather than Pa. The Virial stress tensor σ_{Virial} is defined as:

$$\sigma_{\text{Virial}_{ij}} = \frac{1}{\Omega}\left[-m_i u_i \otimes u_i + \frac{1}{2}\sum_{j\neq i} r_{ij} \otimes f_{ij}\right] \tag{4.2}$$

  where Ω is the volume, m_i is the mass of atom i, u_i is its velocity vector, r_{ij} is the position vector, and f_{ij} is the interatomic force.

- **Strain Calculation:** Engineering strain (ε) was computed from the instantaneous change in the simulation box length (L_x) relative to the original equilibrium length (L_{x0}) in the direction of loading:

$$\varepsilon = \frac{L_x - L_{x0}}{L_{x0}} \tag{4.3}$$

4.2 LAMMPS: Simulation Setup and Loading Protocol

Simulation Initialization and Relaxation

The initial geometry was prepared through a two-step relaxation process:

- **Energy Minimization (CG):** The defective supercells were minimized using the Conjugate Gradient (CG) algorithm to remove structural instability and residual internal stresses. Minimization was run until force and energy tolerances reached 10^{-6} and 10^{-8}, respectively.

- **Thermal Equilibration (NPT/NVT):** The system was equilibrated to the room temperature (300 K) using the NPT (Isothermal-Isobaric) ensemble for 500 ps. A Nosé–Hoover thermostat and barostat were used with damping constants set to 20 ps. An intermediate ramp up to 450 K may be used during equilibration to accelerate the thermal steady state before stabilizing at 300 K.

- **Timestep:** A constant timestep of 1 fs (0.001 ps) was employed for numerical stability throughout all phases.

Uniaxial Tensile Loading (NPT Ensemble)

Uniaxial tensile deformation was applied using a constant engineering strain rate.

- **Ensemble:** The deformation was carried out under the NPT ensemble, maintaining 300 K temperature. The system maintained constant particle number and pressure, allowing the simulation box to expand solely in the direction of applied tension.
- **Strain Rate:** A constant strain rate of 1×10^{8} s^{-1} (or 1×10^{-4} ps^{-1} in fractional units) was imposed. This typical high MD strain rate is commonly employed due to its computational efficiency in capturing material failure events while maintaining reasonable accuracy in simulating TMD failure mechanisms.
- **Anisotropic Loading Rationale:** Tensile loading was performed independently along the Armchair (X-axis) and Zigzag (Y-axis) directions to fully characterize the material's anisotropy (Figure 4.1). This directional testing is critical, as the bond angles and packing density differ significantly in WSe_2 between these axes. While studies on pristine WSe_2 sometimes indicate higher strength along the armchair direction, the introduction of pit defects shifts the failure mechanism, requiring separate analysis of the superior mechanical resistance provided by the zigzag orientation in the defected WSe_2 sheets.

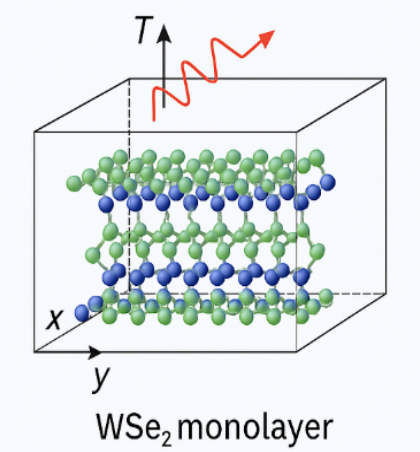

Figure 4.1: WSe_2 Monolayer Conditions

Chapter 5

Results and Discussion

The stress–strain curves obtained from the molecular dynamics simulations of WSe_2 under uniaxial tensile loading reveal the critical mechanical behaviors of the material. For all tested configurations, the curves consistently exhibited an initial linear elastic region, indicative of the material's stiffness, followed by a nonlinear regime, and culminating in a sudden stress drop that signifies crack initiation and catastrophic failure. This sharp decline confirms the material's characteristic brittle failure under tension. The analysis below utilizes data acquired via the Virial stress formalism and visualizations performed using the `OVITO` software to thoroughly characterize the deformation modes and fracture growth behavior.

5.1 Validation of the Simulation Model

To ensure the computational approach's reliability and the accuracy of the employed `Stillinger–Weber (SW)` interatomic potential, the mechanical response of the pristine WSe_2 nanosheet was validated against established literature data under uniaxial tensile loading along the zigzag direction (Figure 5.1).

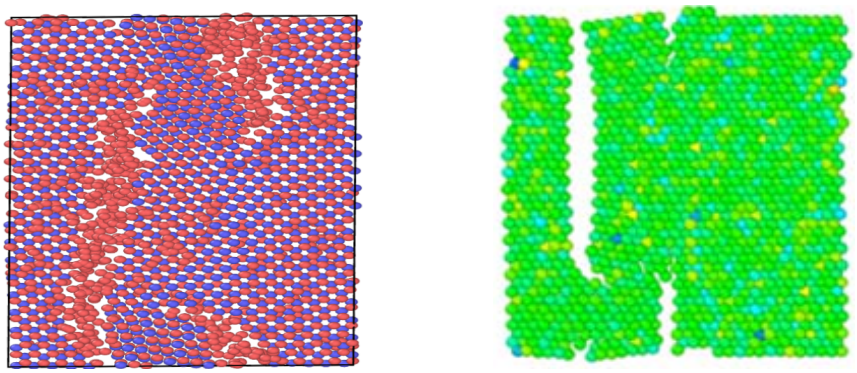

Figure 5.1: Crack Propagation on Pristine nanosheet

The results demonstrated a close correspondence between the calculated and reference values:

- **Maximum Yield Stress (σ_{UTS}):** The present simulation predicted a maximum yield stress of 5.91 GPa. This is in close agreement with the reference value of 5.45 GPa [2, 3].
- **Fracture Strain (ε_f):** The fracture strain was calculated to be approximately 13.45% (0.0791 strain), correlating well with the reference value of 12.91% (0.0711 strain).

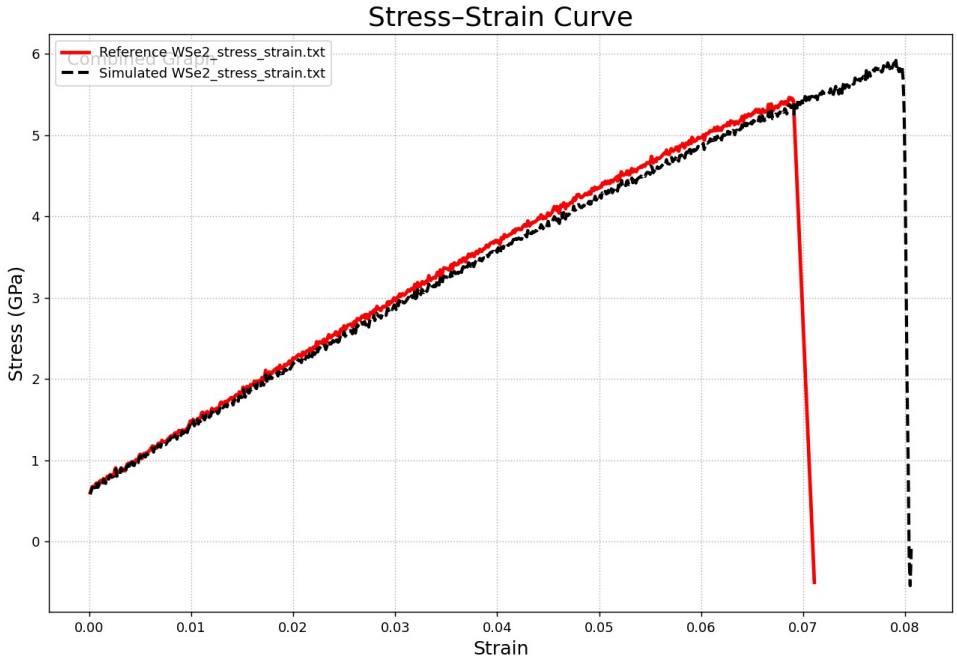

Figure 5.2: Crack propagation graph of Simulated (Black) & Reference (Red) WSe_2

The simulation confirmed that the crack patterns obtained from the initial fracture of the pristine nanosheet also demonstrated consistent fracture mechanisms with the reference study (Figure 5.2), verifying that the developed atomistic model and the applied loading methodology are capable of accurately reproducing the mechanical response of WSe_2. Figure 10 illustrates the comparative stress–strain graph, confirming the validity of the model.

5.2 Crack Propagation on Defected Nanosheet

The MD simulation protocol ensured that the nanosheet underwent deformation and eventual fracture under controlled conditions (300 K temperature, 1×10^8 s^{-1} strain rate, NPT ensemble). The crack propagation analysis demonstrated that both the loading direction (anisotropy) and the geometry of the pit (stress concentration) significantly dictate the structural reliability of WSe_2 for flexible wearable sensors. The fundamental finding is that the zigzag orientation provides

superior mechanical resistance and that circular pits consistently outperform triangular pits in both orientations.

Visualization and Fracture Mechanism Analysis (OVITO)

The atomic configurations and failure pathways were analyzed using the OVITO software. The use of this tool was essential for providing atomistic insight into the macroscopic results.

- **Stress Mapping and Distribution:** Per-atom stress components, calculated via the Virial stress theorem, were imported and mapped onto individual atoms using a color scale. This visualization confirmed that local stress concentrated strongly at the sharp corners of the triangular pits during tensile loading, acting as primary fracture initiation sites.
- **Crack Initiation and Propagation Tracking:** OVITO was used to track the path of bond breaking, confirming that crack nucleation occurred prematurely at the sharp corners of triangular pits or symmetrically around circular pits (Figure 5.3 and 5.4). The software pinpointed the exact simulation step and strain value (ε) for the first atomic bond rupture.
- **Anisotropic Fracture Mechanism:** Sequential atomic snapshots captured via OVITO confirmed the differences in propagation patterns between armchair and zigzag loading. Crucially, complex atomic rearrangements were observed during zigzag loading. In this direction, WSe_2 is prone to lattice phase transformation from the trigonal prismatic phase (h-phase) to the distorted octahedral phase (t-phase). This transformation involves the formation of new W–Se bonds and the appearance of trigon and tetragon structures, which impedes crack propagation, thus explaining the superior fracture resistance and higher fracture strain observed under zigzag loading.
- **Vector Displacement Analysis:** Displacement vectors were rendered to understand the material's elastic response around the pit. For uniaxial loading of triangular pits, vectors near the base pointed inward toward the center. This visualization aids in explaining the macroscopic property differences compared to biaxial loading (as discussed in the $MoTe_2$ context), where displacement vectors extended outward and exhibited directions perpendicular to the pit sides, resulting in a higher Young's modulus but lower fracture strain.

5.2.1 Circular Pitted (Defected) Nanosheet

The circular pit, defined by an isotropic 5 nm diameter, demonstrated superior mechanical robustness across both crystallographic orientations, owing to its ability to distribute stress more uniformly along the curved defect boundary.

- **Zigzag Direction Loading:** When strained along the zigzag direction (the superior orientation), the circular pit system reached a maximum yield strength of 4.079 GPa at a critical strain of 0.0525 ($\approx$ 6.0%). Crack initiation was substantially delayed, occurring at simulation step 1765. This delayed failure suggests that circular geometries significantly enhance the structural resilience of the WSe_2 nanosheet. (Figure 5.3 (a) illustrate the fracture evolution and stress–strain profile).

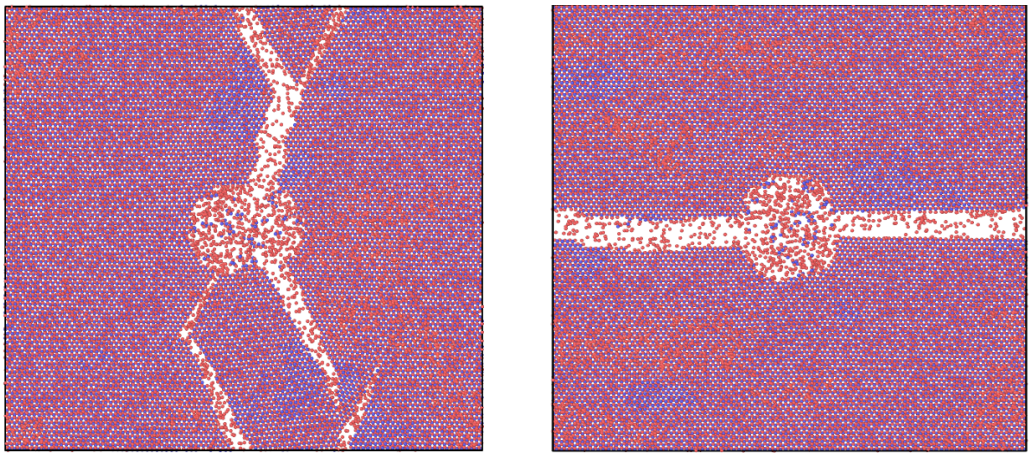

(a) ***Zigzag Direction*** (b) ***Armchair Direction***

Figure 5.3: Crack propagation of Circular Pitted WSe_2 supercells

- **Armchair Direction Loading:** Under armchair loading, the circular pit maintained superior resistance compared to its triangular counterpart. It achieved a maximum yield strength of 3.548 GPa at a strain of 0.0428 ($\approx$ 6.3%). Crack generation initiated at simulation step 1444. Although the overall strength was lower than under zigzag loading, the circular pit still exhibited higher critical strain and greater stability than the triangular pit in this orientation. (Figure 5.3 (b) illustrate the fracture evolution and stress–strain profile).

5.2.2 Triangular Pitted (Defected) Nanosheet

The equilateral triangular pit (5 nm side length) consistently resulted in premature fracture due to high stress localization at its sharp corners, confirming that angular geometries cause localized stress accumulation which accelerates bond rupture.

- **Zigzag Direction Loading:** Despite the overall superiority of the zigzag orientation, the triangular pit system fractured prematurely. It attained a maximum yield strength of only 3.002 GPa at a low strain of 0.0352 ($\approx$ 4.8%). Crack initiation occurred much earlier than the circular pit, specifically at simulation step 1191. The visualization confirmed that cracks originated directly from the sharp tips of the triangular void (Figure 5.4 (a) illustrate the fracture evolution and stress–strain profile).

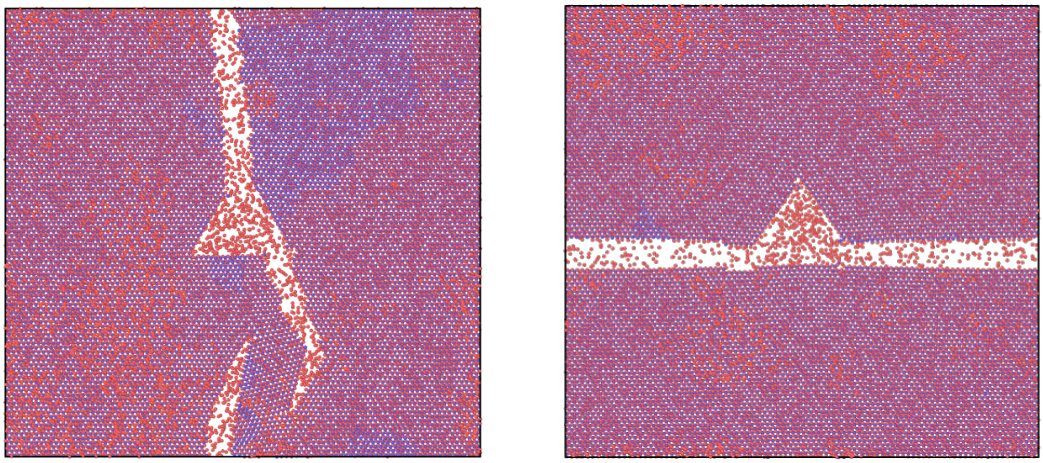

(a) ***Zigzag Direction*** (b) ***Armchair Direction***

Figure 5.4: Crack propagation of Triangular Pitted WSe_2 supercells

- **Armchair Direction Loading:** The detrimental effect of the triangular geometry was exacerbated under armchair loading. Fracture occurred at a maximum yield strength of 3.056 GPa and a minimal strain of 0.0346 ($\approx$ 4.05%). The earliest crack generation step recorded for any defect type was observed here, at step 1162. The visualization confirmed that the reduced failure strain demonstrates the detrimental effect of angular geometries, where localized stress accumulation accelerates bond rupture and leads to premature crack propagation (Figure 5.4 (b) illustrate the fracture evolution and stress–strain profile).

Summary of Defect and Orientation Effects

The overall results, summarized in the comparative tables (Table 5.1 and Table 5.2), clearly reveal the anisotropic nature of WSe_2 and demonstrate that both defect geometry and loading direction significantly alter mechanical performance. The critical findings are:

Table 5.1: Fracture data of Pitted WSe_2 in Zigzag Direction

Aspect	**Circular Pit**	**Triangular Pit**
Maximum Yield Strength (GPa)	4.079	3.002
Crack Propagation Step	1765	1191
Strain at Propagation (ε_f)	0.0525 (6.0%)	0.0352 (4.8%)

Table 5.2: Fracture data of Pitted WSe_2 in Armchair Direction

Aspect	**Circular Pit**	**Triangular Pit**
Maximum Yield Strength (GPa)	3.548	3.056
First Crack Generation Step	1444	1162
Strain at Propagation (ε_f)	0.0428 (6.3%)	0.0346 (4.05%)

1. **Directionality:** Zigzag loading consistently resulted in higher maximum strength than armchair loading, highlighting the structural advantage of zigzag-oriented bonds in distributing stress and accommodating potential phase transformations under strain (as shown in Figure 5.5).

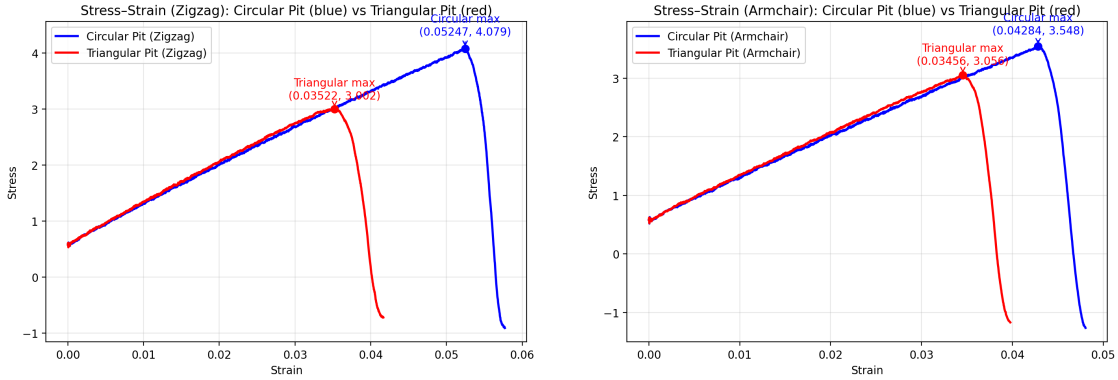

(a) ***Zigzag*** (b) ***Armchair***

Figure 5.5: Graph pf crack propagation in zigzag and armchair direction of Pitted WSe_2 supercells

2. **Defect Geometry:** Circular pits (4.079 GPa max) consistently offered higher load-bearing capacity and delayed crack initiation compared to triangular pits (3.002 GPa max), confirming that eliminating sharp geometric discontinuities is crucial for maintaining the mechanical integrity of WSe_2 nanosheets for flexible sensors.

Chapter 6

Conclusion

The mechanical behavior of monolayer WSe_2 nanosheets containing nanoscale circular and triangular defects was comprehensively characterized through molecular dynamics simulations. The study confirmed that the material exhibits an anisotropic fracture mechanism, with the zigzag orientation offering superior mechanical resistance compared to the armchair direction. Crucially, findings demonstrated that circular defects confer greater strain tolerance and stability (e.g., 4.079 GPa at 6.0% strain for zigzag loading) than triangular defects, which accelerate premature crack initiation due to concentrated local stress at sharp corners. These insights are vital for reliability assessments and defect engineering in flexible nanoelectromechanical systems.

6.1 Future Works

Future research should focus on expanding the scope of these findings to facilitate their application in real-world technologies, particularly addressing the recognized necessity for more comprehensive material comparisons and establishing integration opportunities within the industry. Further investigation is needed to thoroughly characterize the thermal response of tungsten diselenide (WSe_2) under various heat conditions, a key aspect often lacking in previous studies, and to analyze the effect of different defect characteristics to enhance the thermomechanical performance of these materials for flexible wearable sensors. The current mechanical characterization—specifically concerning defect geometry and directional sensitivity—provides valuable guidance for future defect engineering efforts and reliability assessments of two-dimensional transition metal dichalcogenides (TMDs) in nanoelectromechanical systems, and for the rational design of advanced composite structures like graphene/WSe_2 heterostructures for applications in energy storage, catalysis, and electronics.

6.2 Limitations

The inherent limitations of the molecular dynamics methodology must be considered when evaluating the generality of these results. A primary constraint is the use of an extremely high constant engineering strain rate, typically set at 1×10^8 s^{-1} (or 1×10^{-4} ps^{-1}), which is necessitated by computational efficiency but is orders of magnitude faster than actual experimental deformation rates. Although this high simulation rate is effective for capturing material failure events quickly, it may influence the kinetic aspects of crack propagation and bond rupture observed. Furthermore, the detailed quantitative analysis of mechanical properties was specific to the engineered through-hole defects employed—namely, the 5 nm diameter circular pits and the 5 nm side length equilateral triangular pits. Because the mechanical response of TMDs is known to be highly sensitive to precise defect characteristics such as size, concentration, and geometry, the numerical outcomes derived from these specific models should not be universally generalized to all possible defect types without further simulation or experimental validation.

References

[1] M. J. Aziz, M. A. Islam, M. R. Karim, and A. A. Bhuiyan. Effect of triangular pits on the mechanical behavior of 2d mote2: a molecular dynamics study. *Journal of Molecular Modeling*, 30(11):391, 2024.

[2] E. H. Chowdhury, M. H. Rahman, S. Fatema, and M. M. Islam. Investigation of the mechanical properties and fracture mechanisms of graphene/wse2 vertical heterostructure: A molecular dynamics study. *Computational Materials Science*, 188:110231, 2021.

[3] W. Ding, D. Han, J. Zhang, and X. Wang. Mechanical responses of wse2 monolayers: a molecular dynamics study. *Materials Research Express*, 6(8):085071, 2019.

[4] Joseph Falson, Yong Xu, Menghan Liao, Yunyi Zang, Kejing Zhu, Chong Wang, Zetao Zhang, Hongchao Liu, Wenhui Duan, Ke He, Haiwen Liu, Jurgen H. Smet, Ding Zhang, and Qi-Kun Xue. Type-ii ising pairing in few-layer stanene. *Science*, 367(6485):1454–1457, 2020.

[5] L. Fusco, A. Gazzi, G. Peng, Y. Shin, S. Vranic, D. Bedognetti, F. Vitale, A. Yilmazer, X. Feng, B. Fadeel, C. Casiraghi, and L. Delogu. Graphene and other 2d materials: a multidisciplinary analysis to uncover the hidden potential as cancer theranostics. *Theranostics*, 10(12):5435–5488, 2020.

[6] V. Gautam, SK. Verma, R. Singh, Z. Ashraf, K. Kandpal, and P. Kumar. Quasi-2d material based heterostructure devices and its applications. *Journal of Physics D: Applied Physics*, 57(44):443002, 2024.

[7] H. Li, J. Wu, Z. Yin, and H. Zhang. Preparation and applications of mechanically exfoliated single-layer and multilayer mos2 and wse2 nanosheets. *Accounts of chemical research*, 47(4):1067–1075, 2014.

[8] M. Wen, S. N. Shirodkar, P. Plecháč, E. Kaxiras, R. S. Elliott, and E. B. Tadmor. A force-matching stillinger-weber potential for mos2: Parameterization and fisher information theory-based sensitivity analysis. *Journal of Applied Physics*, 122(24), 2017.

[9] Z. Zheng, T. Zhang, J. Yao, Y. Zhang, J. Xu, and G. Yang. Flexible, transparent and ultra-broadband photodetector based on large-area wse2 film for wearable devices. *Nanotechnology*, 27(22):225501, 2016.

Appendix A

LAMMPS Script Snippets

LAMMPS Script Snippets for Loading and Data Output:

The loading command forces the simulation box to deform at the specified rate in the loading direction (X or Y).

```
Line
1   # Apply constant strain rate deformation
2   # Note: For X-axis loading (Armchair)
3   fix 1 all npt temp 300.0 300.0 0.1 x 0.0 0.0 1.0 y 0.0 0.0 1.0 z
    0.0 0.0 0.1
4   fix def all deform 1 x erate 1e-8 units box remap x

5   # Example for data output (adjust frequency as needed)
6   thermo 100
7   thermo_style custom step temp press pxx pyy pzz lx ly lz etotal
8   dump 2 all custom 100 data/output_crack.lammpstrj id type x y z fx fy
    fz c_stress c_stress
```

The dump command records atomic positions (`x, y, z`), forces (`fx, fy, fz`), and per-atom stress components (`c_stress` for σ_{xx}, `c_stress` for σ_{yy}) every 100 steps for post-analysis.